Identification and quantitation of benzo[a]pyrene-DNA adducts formed by rat liver microsome. in vitro

ARTICLE *in* CHEMICAL RESEARCH IN TOXICOLOGY · MARCH 1992

Impact Factor: 3.53 · DOI: 10.1021/tx00026a024 · Source: PubMed

8 AUTHORS, INCLUDING:

Eleanor G Rogan
University of Nebraska at Lincoln
214 PUBLICATIONS **9,004** CITATIONS
SEE PROFILE

Ryszard Jankowiak
Kansas State University
194 PUBLICATIONS **4,765** CITATIONS
SEE PROFILE

pyrene 7,8-diol-9,10-epoxides to DNA, RNA and protein of mouse skin occurs with high stereoselectivity. *Science (Washington, D.C.)* **199**, 778-781.
(10) Rogan, E. G., RamaKrishna, N. V. S., Higginbotham, S., Cavalieri, E. L., Jeong, H., Jankowiak, R., and Small, G. J. (1990) Identification and quantitation of 7-(benzo[a]pyren-6-yl)guanine in the urine and feces of rats treated with benzo[a]pyrene. *Chem. Res. Toxicol.* **3**, 441-444.
(11) Rogan, E., Cavalieri, E., Tibbels, S., Cremonesi, P., Warner, C., Nagel, D., Tomer, K., Cerny, R., and Gross, M. (1988) Synthesis and identification of benzo[a]pyrene-guanine nucleoside adducts formed by electrochemical oxidation and by HRP catalyzed reaction of benzo[a]pyrene with DNA. *J. Am. Chem. Soc.* **110**, 4023-4029.
(12) *NIH Guidelines for the Laboratory Use of Chemical Carcinogens* (1981) NIH Publication No. 81-2385, U.S. Government Printing Office, Washington, DC.
(13) RamaKrishna, N. V. S., Cavalieri, E. L., Rogan, E. G., Dolinkowski, G., Cerny, R. L., Gross, M. L., Jeong, H., Jankowiak, R., and Small, G. J. (1992) Synthesis and structure determination of the adducts of the potent carcinogen 7,12-dimethylbenz[a]anthracene and deoxyribonucleosides formed by electrochemical oxidation: Models for metabolic activation by one-electron oxidation. *J. Am. Chem. Soc.* (in press).
(14) Cavalieri, E., and Calvin, M. (1971) Photochemical coupling of benzo[a]pyrene with 1-methylcytosine: Photoenhancement of carcinogenicity. *Photochem. Photobiol.* **14**, 641-653.
(15) Jeffrey, A. M., Grzeskowiak, K., Weinstein, I. B., Nakanishi, K., Roller, P., and Harvey, R. G. (1979) Benzo(a)pyrene-7,8-dihydrodiol 9,10-oxide adenosine and deoxyadenosine adducts: Structure and stereochemistry. *Science (Washington, D.C.)* **206**, 1309-1311.

Identification and Quantitation of Benzo[*a*]pyrene–DNA Adducts Formed by Rat Liver Microsomes in Vitro

P. D. Devanesan,[†] N. V. S. RamaKrishna,[†] R. Todorovic,[†] E. G. Rogan,*[,†] E. L. Cavalieri,[†] H. Jeong,[‡] R. Jankowiak,[‡] and G. J. Small[‡]

Eppley Institute for Research in Cancer and Allied Diseases, University of Nebraska Medical Center, 600 South 42nd Street, Omaha, Nebraska 68198-6805, and Department of Chemistry and Ames Laboratory—USDOE, Iowa State University, Ames, Iowa 50011

Received September 9, 1991

The two DNA adducts of benzo[a]pyrene (BP) previously identified in vitro and in vivo are the stable adduct formed by reaction of the bay-region diol epoxide of BP (BPDE) at C-10 with the 2-amino group of dG (BPDE-10-N^{2}dG) and the adduct formed by reaction of BP radical cation at C-6 with the N-7 of Gua (BP-6-N7Gua), which is lost from DNA by depurination. In this paper we report identification of several new BP–DNA adducts formed by one-electron oxidation and the diol epoxide pathway, namely, BP bound at C-6 to the C-8 of Gua (BP-6-C8Gua) and the N-7 of Ade (BP-6-N7Ade) and BPDE bound at C-10 to the N-7 of Ade (BPDE-10-N7Ade). The in vitro systems used to study DNA adduct formation were BP activated by horseradish peroxidase or 3-methylcholanthrene-induced rat liver microsomes, BP 7,8-dihydrodiol activated by microsomes, and BPDE reacted with DNA. Identification of the biologically-formed depurination adducts was achieved by comparison of their retention times on high-pressure liquid chromatography in two different solvent systems and by comparison of their fluorescence line narrowing spectra with those of authentic adducts. The quantitation of BP–DNA adducts formed by rat liver microsomes showed 81% as depurination adducts: BP-6-N7Ade (58%), BP-6-N7Gua (10%), BP-6-C8Gua (12%), and BPDE-10-N7Ade (0.5%). Stable adducts (19% of total) included BPDE-10-N^{2}dG (15%) and unidentified adducts (4%). Microsomal activation of BP 7,8-dihydrodiol yielded 80% stable adducts, with 77% as BPDE-10-N^{2}dG and 20% of the depurination adduct BPDE-10-N7Ade. The percentage of BPDE-10-N^{2}dG (94%) was higher when BPDE was reacted with DNA, and only 1.8% of BPDE-10-N7Ade was obtained. Activation of BP by horseradish peroxidase afforded 32% of stable unidentified adducts and 68% of depurination adducts, with 48% of BP-6-N7Ade, 9% of BP-6-N7Gua, and 11% of BP-6-C8Gua. These results show that with activation by cytochrome P-450 the BP–DNA adducts are predominantly formed by one-electron oxidation and lost from DNA by depurination.

Introduction

Covalent binding of polycyclic aromatic hydrocarbons (PAH)[1] to target cell DNA is thought to be the first event in the tumor-initiating process. The physicochemical properties of PAH and the catalytic properties of cytochrome P-450s suggest that PAH are generally activated by two major mechanisms, one-electron oxidation with formation of radical cations (*1*, *2*) and monooxygenation to yield bay-region diol epoxides (*3*, *4*). Some PAH are thought to be activated by the diol epoxide pathway alone, others by one-electron oxidation alone, and some by a

* To whom correspondence should be addressed.
[†] University of Nebraska Medical Center.
[‡] Iowa State University.

[1] Abbreviations: BP, benzo[a]pyrene; BPDE, (+)-*r*-7,*t*-8-dihydroxy-*t*-9,10-epoxy-7,8,9,10-tetrahydrobenzo[a]pyrene (anti); BP-6-N7Ade, 7-(benzo[a]pyren-6-yl)adenine; BP-6-N7Gua, 7-(benzo[a]pyren-6-yl)-guanine; BP-6-C8Gua, 8-(benzo[a]pyren-6-yl)guanine; BP-6-C8dG, 8-(benzo[a]pyren-6-yl)deoxyguanosine; BPDE-10-N^{2}dG, 10-(deoxyguanosin-*N*^{2}-yl)-7,8,9-trihydroxy-7,8,9,10-tetrahydrobenzo[a]pyrene; BPDE-10-N7Gua, 10-(guanin-7-yl)-7,8,9-trihydroxy-7,8,9,10-tetrahydrobenzo[a]pyrene; BPDE-10-N7Ade, 10-(adenin-7-yl)-7,8,9-trihydroxy-7,8,9,10-tetrahydrobenzo[a]pyrene; clotrimazole, 1-(*o*-chloro-α,α-diphenylbenzyl)imidazole; DMSO, dimethyl sulfoxide; DPEA, 2-[(4,6-dichlorobiphenyl-2-yl)oxy]ethylamine hydrobromide; FLN, fluorescence line narrowing; FLNS, fluorescence line narrowing spectroscopy; HPLC, high-pressure liquid chromatography; PAH, polycyclic aromatic hydrocarbon(s).

0893-228x/92/2705-0302$03.00/0

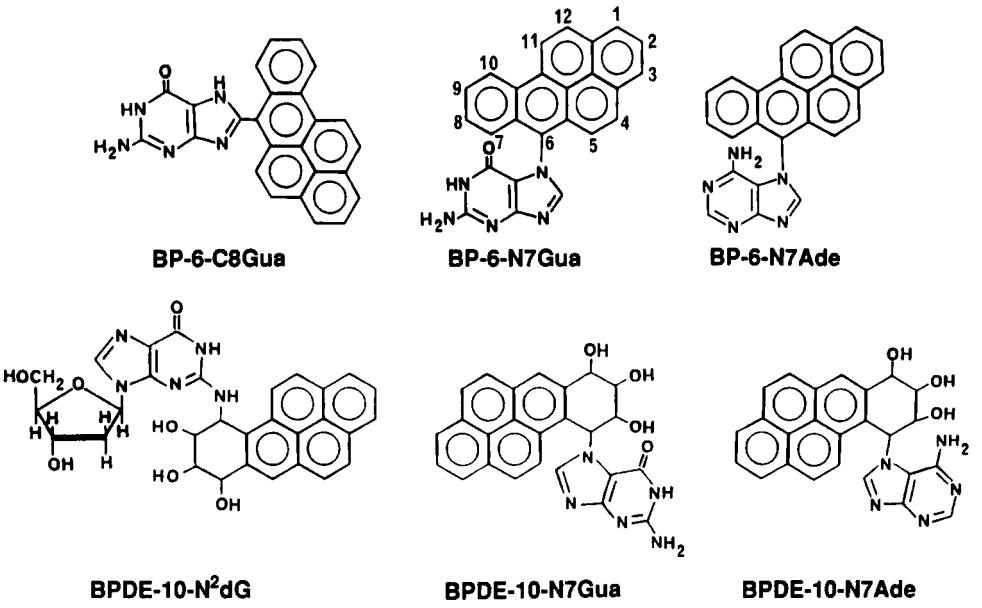

Figure 1. Structures of adducts analyzed.

combination of both pathways. This overall view of PAH activation is based on several different types of results, including tumorigenicity data and the structure of PAH–DNA adducts.

Identification of PAH–DNA adducts can reveal the mechanism of activation. The possibility to understand the biological significance of PAH adduction to DNA relies, however, not only on identification of the adducts but also on their quantitation. In addition, one must examine not only PAH–DNA adducts that remain stable in DNA but also adducts that are lost from the DNA by depurination.

Two DNA adducts of benzo[*a*]pyrene (BP) have been reported to be formed in vitro in reactions catalyzed by cytochrome P-450. One is the stable adduct formed by reaction of the bay-region diol epoxide of BP (BPDE) at C-10 with the 2-amino of dG (BPDE-10-N^{2}dG, Figure 1) (*5*, *6*); the second one is the adduct formed by reaction of BP radical cation with the N-7 of Gua (BP-6-N7Gua), which is lost from DNA by depurination (*7*). These two adducts have also been identified in vivo, BPDE-10-N^{2}dG in mouse skin (*8*) and BP-6-N7Gua in the urine and feces of rats (*9*).

In this paper we report the identification of several new BP–DNA adducts formed by one-electron oxidation and the diol epoxide mechanism, namely, BP bound at C-6 to the C-8 of Gua (BP-6-C8Gua) and N-7 of Ade (BP-6-N7Ade) and BPDE bound at C-10 to the N-7 of Ade (BPDE-10-N7Ade) (Figure 1). In addition, we report that the comparable adduct of BPDE bound at C-10 to the N-7 of Gua was not observed. The in vitro systems used to study DNA adduct formation were (1) BP activated by 3-methylcholanthrene (MC)-induced rat liver microsomes or horseradish peroxidase (HRP), (2) BP 7,8-dihydrodiol activated by MC-induced rat liver microsomes, and (3) BPDE reacted with DNA. Authentic adducts used in these identifications were previously synthesized and their structures elucidated (*10*, *11*). Identification of the biologically-formed adducts was achieved by comparison of their retention time on high-pressure liquid chromatography (HPLC) in two different solvent systems and by comparison of their fluorescence line narrowed (FLN) spectra (*12*) with those of authentic adducts.

To gain an overall picture of the BP–DNA adducts formed by rat liver microsomes, we have quantitated the stable and depurination adducts formed in each system. This information is a prerequisite for understanding the biological significance of these adducts in initiating cancer.

Materials and Methods

Chemicals. BP-6-C8Gua, BP-6-N7Gua, and BP-6-N7Ade were synthesized by anodic oxidation of BP in the presence of dG or dA (*10*, *11*). BPDE-10-N7Gua and BPDE-10-N7Ade were prepared by chemical reaction of BPDE with dG or dA as reported in the preceding paper (*11*).

[^{3}H]BP (sp act. 550 Ci/mol) was purchased from Amersham (Arlington Heights, IL), whereas [^{3}H]-(+)-*trans*-BP 7,8-dihydrodiol (sp act. 767 Ci/mol) and [^{3}H]-(+)-*r*-7,*t*-8-dihydroxy-t-9,10-epoxy-7,8,9,10-tetrahydro-BP (anti) (sp act. 1380 Ci/mol) were purchased from the NCI Chemical Carcinogen Repository. [^{3}H]BP was used at a specific activity of 410 Ci/mol, [^{3}H]BP 7,8-dihydrodiol at 550 Ci/mol, and [^{3}H]BPDE at 370 Ci/mol. BP, BPDE, and BP 7,8-dihydrodiol are hazardous chemicals; they are handled in accordance with NIH guidelines (*13*).

Binding of PAH to DNA. As previously described (*14*), [^{3}H]BP (80 μM) and [^{3}H]BP 7,8-dihydrodiol (15 μM) were bound to DNA in reactions catalyzed by MC-induced rat liver microsomes, and [^{3}H]BP was also bound to DNA by HRP. BPDE was bound to DNA in a mixture containing 2.6 mM calf thymus DNA in 150 mM Tris-HCl, pH 7.5, 150 mM KCl, 5 mM $MgCl_2$, and 15 μM [^{3}H]BPDE. All of the reactions were 15 mL in volume; they were incubated for 30 min at 37 °C.

At the end of the reaction, a 1-mL aliquot of the mixture was used to determine the level of PAH binding to DNA and the amount of stable adducts by the P_1-nuclease-modified ^{32}P-postlabeling method, as previously described (*14*). The DNA from the remaining 14-mL mixture was precipitated with 2 volumes of absolute ethanol, and the supernatant was used to identify and quantify the depurination adducts by HPLC and FLNS.

Analysis of Depurination Adducts by HPLC and FLNS. The supernatant from each binding reaction, which contained depurination adducts and metabolites, was evaporated to dryness under vacuum. The residue was dissolved in dimethyl sulfoxide (DMSO)/CH_3OH (1:1). After sonication to enhance solubilization, the undissolved residue was removed by centrifugation.

A 75-μL aliquot was analyzed on a YMC 5-μm, ODS-AQ reverse-phase analytical column (6.0 × 250 mm) (YMC, Overland Park, KS) on a Waters 600E multisolvent delivery system together with a Waters 700 satellite WISP autoinjector (Millipore Corp., Wood Dale, IL). The column was eluted for 5 min with 30% CH_3OH in H_2O, followed by an 80-min convex (CV5) gradient to 100% CH_3OH, at a flow rate of 1.0 mL/min. The peaks were detected by UV absorbance (254 nm) using a Waters 990 photodiode array detector and by radioactivity (Radiomatic Flo-one/Beta radiation monitor, A250 series, Radiomatic, Tampa,

Table I. Separation of Adducts by HPLC[a]

adduct	retention time, min		
	A	B	C
BP-6-C8Gua	53.1	33.3	
BP-6-N7Gua	56.8		47.5
BP-6-N7Ade	55.4	35.2	
BPDE-10-N7Gua	44.1		30.2
BPDE-10-N7Ade	41.2		31.3

[a] Gradient A: 30% CH_3OH in H_2O for 5 min, followed by a convex (CV5) gradient to 100% CH_3OH in 80 min at a flow rate of 1.0 mL/min. Gradient B: 30% CH_3CN in H_2O for 5 min, followed by a convex (CV5) gradient to 100% CH_3CN in 75 min at a flow rate of 1.0 mL/min. Gradient C: 20% CH_3CN in H_2O for 5 min, followed by a linear (CV6) gradient to 100% CH_3CN in 80 min at a flow rate of 1.0 mL/min.

FL). The synthesized authentic adducts were used as reference markers. The radioactive adducts coeluting with the authentic adducts were collected in multiple runs. The combined material was evaporated under argon, redissolved in DMSO/CH_3OH (1:1), and further chromatographed on one of two CH_3CN/H_2O gradients. The details of column elution conditions for each adduct are listed in Table I.

For each type of incubation, the depurination adducts were analyzed in four experiments. In a first experiment, the depurination adducts were identified by HPLC in both CH_3OH/H_2O and CH_3CN/H_2O gradients in the presence of added authentic adducts. In a second experiment, the adducts were chromatographed in both solvent systems without added authentic adducts, and the material eluting at the respective retention times on the CH_3CN/H_2O gradient was collected for identification by FLNS. In the third and fourth experiments, quantitative data were collected for calculation of the amounts of both the depurination and stable adducts. The amounts of each adduct varied in the two experiments by 10–25%, with the larger variations in the minor adducts.

Identification of the depurination adducts by FLNS was conducted as previously described (*12*, *15*).

Calculation of Adduct Levels. The amount of stable adducts was calculated by the ^{32}P-postlabeling method as previously described (*14*). For quantitation of the depurination adducts, each of the peaks eluting at the same time as an authentic adduct in HPLC using the CH_3OH/H_2O gradient was collected and counted. These peaks were then reinjected individually in an CH_3CN/H_2O gradient, and the percentage of the injected radioactivity eluting at the same time as the authentic adduct was measured and calculated using the radiation flow monitor. The total amount of each of the adducts was calculated from the specific activity of the PAH and normalized to the amount of DNA used in the reaction.

Effects of Cytochrome P-450 Inhibitors. Each of the cytochrome P-450 inhibitors 2-[(4,6-dichlorobiphenyl-2-yl)oxy]-ethylamine hydrobromide (DPEA) and 1-(*o*-chloro-α,α-diphenylbenzyl)imidazole (clotrimazole) was added to microsomal incubations at various ratios to the substrate, BP, to determine the amount of inhibition of formation of stable adducts. DPEA was used at ratios of 1, 5, and 10 times BP, whereas clotrimazole was 0.2, 1, and 2 times BP. At the highest ratios, i.e., DPEA = 10 × BP and clotrimazole = 2 × BP, 15-mL reaction mixtures were incubated and the amounts of both stable and depurination adducts were determined as described above.

Results and Discussion

Identification of DNA Adducts. To identify the BP–DNA adducts formed by cytochrome P-450 in MC-induced rat liver microsomes, we compared the adducts to those formed by one-electron oxidation of BP, catalyzed by HRP, and those formed by microsomal activation of BP 7,8-dihydrodiol or by reaction of BPDE itself with DNA. The stable adducts were quantitated and partially identified by the ^{32}P-postlabeling technique. The depurination adducts were quantitated and identified by comparison with authentic adducts on HPLC (see Materials and Methods and Table I) and FLNS.

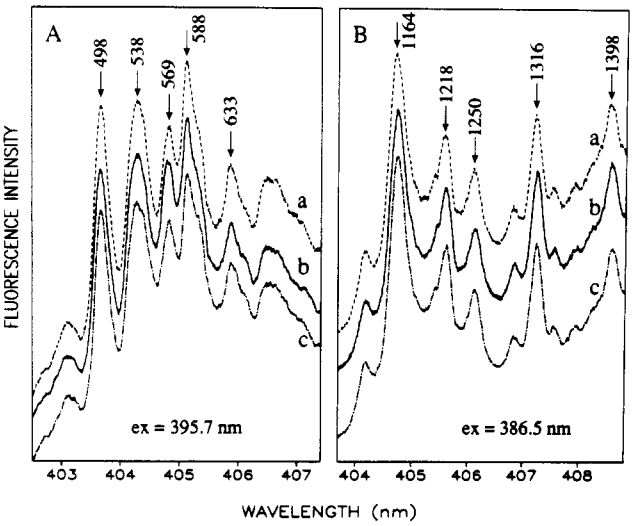

Figure 2. FLN spectrum of the synthesized BP-6-N7Gua (a) [excited with λ_{ex} = 395.7 nm (A) and 386.5 nm (B)] compared to the spectra of BP-6-N7Gua from the HRP reaction (b) and microsomal reaction (c).

Four depurination adducts were identified, BP-6-C8Gua, BP-6-N7Gua, BP-6-N7Ade, and BPDE-10-N7Ade. Preliminary identification of these adducts was made by coelution with authentic adducts on HPLC in two different solvent systems, namely, CH_3OH/H_2O and CH_3CN/H_2O gradients (Table I). Proof of structure was obtained by FLNS analysis. This type of analysis only requires about 1 pg of adduct.

Identification of BP-6-N7Gua by FLN spectra was obtained with two different laser excitations, at 395.7 nm (Figure 2A) and 386.5 nm (Figure 2B). Spectra b and c are virtually indistinguishable and are identical to the FLN spectra of the standard adduct (spectra a). BP-6-N7Gua was previously identified when BP was bound to DNA by HRP (*10*) or rat liver microsomes (*7*). These FLN spectra are also identical to those of the BP-6-N7Gua adduct isolated from the urine and feces of rats treated with BP (*9*).

For both excitations, several strong zero-phonon lines are observed, in which vibrational mode frequencies are significantly perturbed by the substitution of Gua at N-7, compared to the unsubstituted BP chromophore. This is detailed in Table II, a compilation of the excited-state vibrational frequencies for BP and the various adducts. The frequency ranges cover 400–700 and 1100–1400 cm^{-1}, the regions of greatest activity.

Identification of BP-6-C8Gua was also obtained at two excitations, 395.7 nm (Figure 3A) and 386.5 nm (Figure 3B). As in Figure 2, these wavelengths were chosen to reveal mode structure in the 600- and 1200-cm^{-1} regions. Spectra a in Figure 3 were obtained for the standard BP-6-C8Gua adduct and are identical to the FLN spectra reported earlier (*15*). Spectra b, from HRP-catalyzed binding of BP to DNA, and spectra c, from microsome-catalyzed binding, exhibit exactly the same modes as spectra a (e.g., 498, 538, 586, and 1164 cm^{-1}). These data, along with its coelution with authentic adduct on HPLC, demonstrate that this adduct is BP-6-C8Gua.

The major depurination adduct produced by both HRP and microsomes was identified as BP-6-N7Ade. A specific region of the standard FLN spectra, obtained with laser excitation at 386.5 nm, is presented in Figure 4 for (a) the authentic BP-6-N7Ade, (b) adduct from the HRP-cata-

Table II. Excited-State (S_1) Vibrational Frequencies (cm^{-1}) of Depurination Adducts from both One-Electron Oxidation and Monooxygenation Compared to Vibrational Frequencies of BP and *anti-trans*-BP Tetraol[a]

		one-electron oxidation adducts			monooxygenation adducts	
BP	*anti-trans*-BP tetraol	BP-6-N7Gua	BP-6-C8Gua	BP-6-N7Ade	BPDE-10-N7Gua	BPDE-10-N7Ade
327	450	465	469	–	394	394
376	468	498	498	496	469	470
427	577	538	538	–	–	498
449	956	569	563	554	506	510
471	1385	588	586	587	535	543
512	1406	–[b]	–	612	555	565
549	1442[c]	633	–	634	578	580
580	1500	671	–	–	**610**[d]	**606**[d]
624	1517	1132	1126	1132	957	957
686	1559	1164	1164	1164	1005	1009
750		1218	1219	1220	1044	1045
789		1250	1247	1252	–	1079
837		1296	–	–	1119	1110
912		1316	1314	1316	1122	1122
921		1398	–	1396	1176	1176
933					1246	~1246
954					1262	1262
973					1306[d]	1293[d]
1009					1333	1333
1032					1367	1368
1063					1388	1385
1119					1443	1442
1133					1464	1466
1179					1505	1505[e]
					1518	1518
					1561	1561
					1603	1603

[a] Excitation wavelengths used: for one-electron oxidation adducts, 386.5 and 395.7 nm; for monooxygenation adducts, 356.9, 359.6, 363.4, 369.6, and 371.6 nm; for *anti-trans*-BP tetraol, 356.9, 363.4, 369.6, and 371.6 nm; for BP, 386.5, 392, and 393.8 nm. [b] (–) Not observed or very weak. [c] Strongest mode for 356.9-nm excitation; 1517- and 1559-cm^{-1} modes for this excitation are weak. [d] 610 and 606 cm^{-1} (or 1306 and 1293 cm^{-1}) can be used to differentiate between BPDE-10-N7Gua and BPDE-10-N7Ade. The 606-cm^{-1} mode is pronounced while the 610-cm^{-1} mode is weak (369.6-nm excitation). [e] Pronounced shoulder for 356.9-nm excitation; better resolved for λ_{ex} = 359.6 nm, see Figure 6.

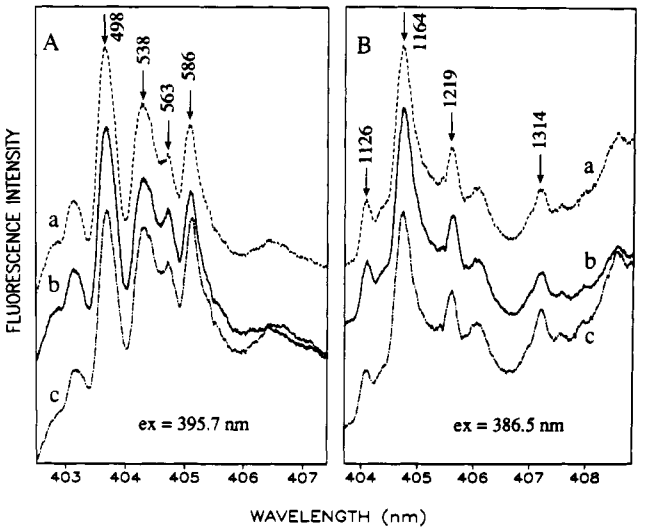

Figure 3. FLN spectrum of the synthesized BP-6-C8Gua (a) [excited with λ_{ex} = 395.7 nm (A) and 386.5 nm (B)] compared to the spectra of BP-6-C8Gua from the HRP reaction (b) and microsomal reaction (c).

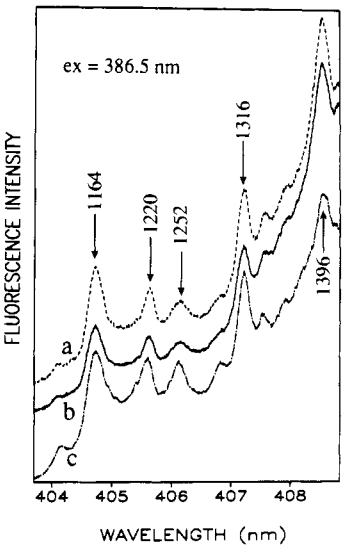

Figure 4. Comparison of the vibronically excited FLN spectra (λ_{ex} = 386.5 nm) of the synthesized BP-6-N7Ade (a) and BP-6-N7Ade from the HRP reaction (b) and microsomal reaction (c).

lyzed binding, and (c) adduct from the microsomal reaction. Spectra a–c are virtually indistinguishable, and it is apparent that the adduct formed by HRP or microsomes is BP-6-N7Ade. Additional support for this assignment (and others) is provided by FLN spectra obtained with other excitation wavelengths (data not shown).

From the FLN spectra discussed above (Figures 2–4 and Table II) and others obtained with different excitation wavelengths, it is apparent that the vast majority of the excited-state mode frequencies for BP-6-N7Gua, BP-6-C8Gua, and BP-6-N7Ade are identical within experimental uncertainty (±2 cm^{-1}). There are, however, two notable exceptions: the 569- and 1132-cm^{-1} modes of BP-6-N7Gua, which have the values (563, 1126) and (554, 1132) cm^{-1} for BP-6-C8Gua and BP-6-N7Ade, respectively. Nevertheless, the ability of FLNS to distinguish convincingly between the three adducts rests on the fact that the S_1 (fluorescent) state of BP-6-N7Ade lies about 100 cm^{-1} lower in energy than that of BP-6-N7Gua, which, in turn, lies another 100 cm^{-1} lower than BP-6-C8Gua. This state ordering was determined from 77 K non-line narrowed fluorescence spectra (not shown). The S_1-state energy shifts are re-

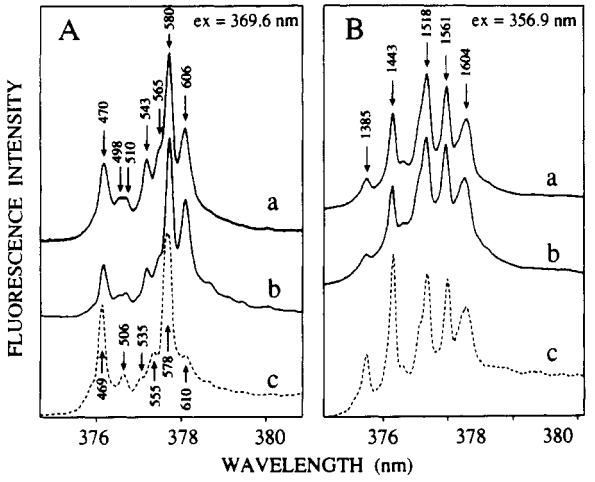

Figure 5. Difference FLN spectra excited with λ_{ex} = 369.6 nm (A) and 356.9 nm (B) of the synthesized BPDE-10-N7Ade (b) and BPDE-10-N7Gua (c) adducts compared to the spectrum of BPDE-10-N7Ade from the microsomal reaction (a). Gated detection with suitable delay was employed (see text). Note that the 470-, 580-, 1385-, and 1443-cm^{-1} bands for the microsomal depurination adduct (a) are slightly contaminated by tetraols; see text for discussion.

sponsible for the distinct vibronic intensity distributions observed for each adduct for every *vibronic* excitation wavelength used (see ref 12 for a detailed discussion). Indeed, the above state ordering can be deduced from the FLN spectra shown (*12*).

Finally, a depurination adduct formed from BPDE was identified as BPDE-10-N7Ade. For this adduct four different excitation wavelengths were employed. The results for 369.6 and 356.9 nm are shown in Figure 5, panels A and B, respectively. Spectrum a for both is for the adduct isolated from the microsome-catalyzed reaction with BP while spectra b and c are for the BPDE-10-N7Ade and BPDE-10-N7Gua standards, respectively. Although the standard adducts were purified by HPLC, their FLN spectra were found to be contaminated by tetraol emission, indicating that both adducts are unstable. To minimize the effect of the tetraol, gated detection with suitable delay was employed (see below). We note first that the excited-state mode frequencies for the microsomal adduct (a) and the synthesized BPDE-10-N7Ade standard (b) are identical within experimental uncertainty. There are minor differences, however, in the vibronic intensity distributions, which were found to depend on the delay time of the gate (for comparison, see the near-perfect agreement in vibronic intensities for the in vitro and standard adducts shown in Figures 2–4). The tendency of BPDE-type adducts to undergo hydrolysis and photochemical decomposition to yield tetraol is well-known, and given the high fluorescence quantum yields of tetraols, great care must be exercised in order not to misassign tetraol fluorescence to BPDE-type adducts (*16*). Fortunately, the tetraols have a relatively long fluorescence lifetime (≥200 ns) compared to the adducts (~150 ns) so that time resolution can be used to discriminate partially against tetraols of BPDE. The spectra shown in Figure 5, panels A and B, represent the difference of two spectra obtained with gate delays of 30 and 125 ns. The gate width used was 100 ns. Especially for λ_{ex} = 369.6 nm (Figure 5A), there is good agreement between the vibronic intensities of the microsomal adduct and BPDE-10-N7Ade. For both λ_{ex} values, spectra a in Figure 5 show significantly better agreement for BPDE-10-N7Ade than for BPDE-10-N7Gua. Notably, the 610-cm^{-1} band of the latter is markedly weaker and shifted by 4 cm^{-1} relative to the 606-cm^{-1} band for the microsomal

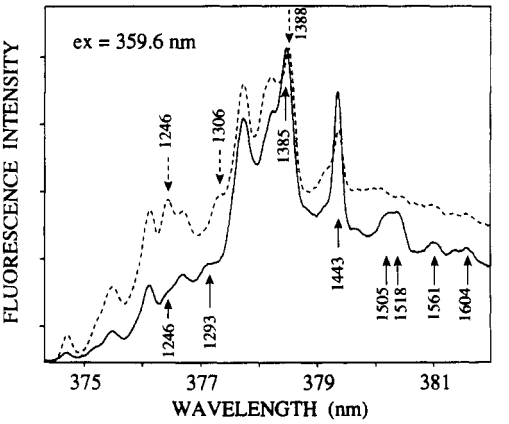

Figure 6. Difference FLN spectra (obtained as in Figure 5) of BPDE-10-N7Gua (dashed line) and BPDE-10-N7Ade (solid line) generated at T = 4.2 K with λ_{ex} = 359.6 nm. Note that the S_1 state of BPDE-10-N7Ade lies lower (relative to BPDE-10-N7Gua) in energy by ~100 cm^{-1}.

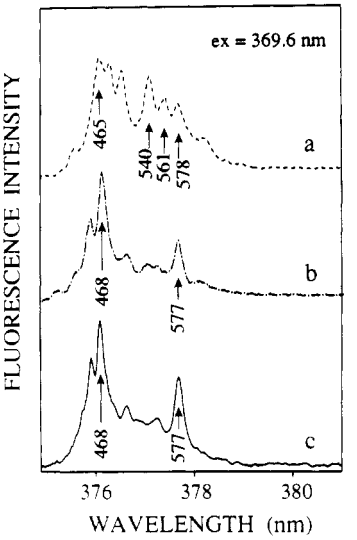

Figure 7. Standard FLN spectra of *cis*- (a) and *trans*-tetraols (b) compared to a hydrolyzed sample of BPDE-10-N7Ade adduct (c). T = 4.2 K, λ_{ex} = 369.6 nm.

and BPDE-10-N7Ade adducts (Figure 5A). Furthermore, the centroid of the vibronic intensity distribution of BPDE-10-N7Gua (Figure 5) lies substantially to the blue (~100 cm^{-1}) of those of the other two. Therefore, on the basis of the FLN spectra and HPLC retention times in two different solvent systems, we conclude that the microsomal adduct is BPDE-10-N7Ade.

Further evidence that FLNS can be used to distinguish between BPDE-10-N7Ade and BPDE-10-N7Gua is provided by the spectra in Figure 6, which were obtained with λ_{ex} = 359.6 nm and are significantly different in their vibronic intensity distributions. The greater intensities of the 1443–1604-cm^{-1} modes but weaker intensities in the ~1250-cm^{-1} region of BPDE-10-N7Ade (solid line) relative to those of BPDE-10-N7Gua (dashed line) should be noted. These differences support the conclusion that the S_1 state of the former lies lower in energy by ~100 cm^{-1}. There are some differences in frequencies as well, e.g., 1306 vs 1293 cm^{-1}. Table II gives a comparison of the excited-state mode frequencies for the two adducts.

We turn now to a more detailed consideration of the FLN spectra of BP tetraols. Spectra a and b of Figure 7 are reproduced from ref 17 and correspond, respectively, to the cis and trans isomers of BP tetraol for λ_{ex} = 369.6 nm. The quite remarkable differences in the vibronic

Table III. Quantitation of Biologically-Formed BP-DNA Adducts[a]

incubation system	total adducts, (mol/mol of DNA-P) × 10^6	stable DNA adducts, (mol of adduct/mol of DNA-P) × 10^6			depurination DNA adducts, (mol of adduct/mol of DNA-P) × 10^6					
		BPDE-10-N^2dG	unidentified	stable adducts, % of total	BPDE-10-N7Ade	BP-6-C8Gua	BP-6-N7Gua	BP-6-N7Ade	depurination adducts, % of total	ratio of depurination/stable
HRP										
BP	21.5		6.9[b] (32)[c]	32		2.3 (11)	1.9 (9)	10.4 (48)	68	2.1
MC-induced microsomes										
BP	18.2	2.7 (15)	0.8[d] (4)	19	0.1 (0.5)	2.2 (12)	1.8 (10)	10.6 (58)	81	4.2
BP 7,8-dihydrodiol	36.4	28.2 (77)	1.1[e] (3)	80	7.1 (20)				20	0.24
BPDE	93.4	87.6 (94)	4.1[f] (4)	98	1.7 (1.8)				1.8	0.02

[a] Values are the average of determinations on two preparations. The amount of each adduct varied between 10 and 25% in the two preparations, with larger variations with the minor adducts. [b] 5 adduct spots. [c] Number in parentheses is percentage of total adducts. [d] 9 adduct spots. [e] 4 adduct spots. [f] 6 adduct spots.

Table IV. Inhibition of Formation of BP-DNA Adducts by Rat Liver Microsomes[a]

	stable DNA adducts, (mol of adduct/mol of DNA-P) × 10^6			depurination adducts, (mol of adduct/mol of DNA-P) × 10^6			
	total stable adducts	BPDE-10-N^2dG	unidentified	BPDE-10-N7Ade	BP-6-C8Gua	BP-6-N7Gua	BP-6-N7Ade
control (BP alone)	2.51	1.79	0.72	0.07	1.58	1.30	7.63
BP							
+1× DPEA[b]	1.58 (38)[c]	1.24 (31)	0.34 (53)				
+5× DPEA	0.19 (93)	0.14 (92)	0.05 (93)				
+10× DPEA	0.025 (99)	0.018 (99)	0.007 (99)	<0.05 (100)	<0.05 (100)	<0.05 (100)	<0.05 (100)
BP							
+0.2× clotrimazole	1.51 (40)	1.06 (41)	0.45 (38)				
+1× clotrimazole	0.90 (64)	0.64 (64)	0.26 (64)				
+2× clotrimazole	0.21 (92)	0.12 (93)	0.09 (88)	<0.05 (100)	<0.05 (100)	<0.05 (100)	<0.05 (100)

[a] Values are the average of detrminations on two preparations. The amount of each adduct varied no more than 10% in the two preparations. [b] The number indicates the molar ratio of inhibitor to BP. [c] The number in parentheses is percent inhibition.

intensity distributions are comparable to those observed for the cis and trans isomers of (+)-*anti*-BPDE–GMP (guanosine monophosphate) (*12*). Spectrum c of Figure 7 corresponds to a hydrolyzed sample of BPDE-10-N7Ade (the spectrum for hydrolyzed BPDE-10-N7Gua is identical; not shown). There is good agreement between spectra b and c, indicating that the BP tetraol formed by hydrolysis of both adducts is the trans isomer. Comparison of spectra b and c (Figure 7) with spectrum b of Figure 5A (BPDE-10-N7Ade) shows that the adduct has minimal BP tetraol contamination. It has been our experience that HPLC-purified BPDE-10-N7Gua and BPDE-10-N7Ade samples decompose over time even when stored at 0 °C. This can be observed from the increased contribution of spectrum b of Figure 7 (*trans*-BP tetraol).

Finally, we remark that minor differences between the FLN vibronic intensity distributions of the microsomal and BPDE-10-N7Ade spectra (Figure 5) could conceivably be attributed to the presence of the cis and trans isomers of *syn*-BPDE adducts in the microsomal sample.

Formation of apurinic sites at guanines in BPDE-treated DNA has been attributed to depurination of BPDE-10-N7Gua (*18*). Therefore, a surprising finding in the analysis of adducts formed by BPDE was the lack of detection of BPDE-10-N7Gua. If this adduct was formed, it was below the level of detection with these experimental procedures, i.e., less than 0.05 (mol/mol of DNA-P) × 10^6.

Quantitation of DNA Adducts. Quantitation of stable adducts was accomplished by the ^{32}P-postlabeling method, whereas quantitation of depurination adducts was conducted by HPLC with a radiation flow monitor.

When BP was activated by rat liver microsomes, the major stable adduct was BPDE-10-N^2dG (15% of total, Table III), whereas the other minor, unidentified stable adducts constituted only 4% of the total. The depurination adducts, namely, BP-6-C8Gua, BP-6-N7Gua, BP-6-N7Ade, and a small amount of BPDE-10-N7Ade (0.5%), were, however, predominant. The three formed by one-electron oxidation, in an approximate molar ratio of 1:1:6, respectively, constituted 81% of the total adducts, with BP-6-N7Ade accounting for 58% by itself.

The same three depurination adducts formed by one-electron oxidation, BP-6-C8Gua, BP-6-N7Gua, and BP-6-N7Ade, were obtained by HRP-catalyzed binding of BP to DNA (Table III). The ratio of these adducts was about 1:1:5, and they constituted 68% of all of the adducts formed. The other 32% were stable, unidentified adducts.

When BP 7,8-dihydrodiol was activated by microsomes, the preponderant adduct was the stable BPDE-10-N^2dG, 77%, and the stable adducts constituted 81% of the total, with the other 19% as the depurination adduct BPDE-10-N7Ade. When BPDE was reacted with DNA, 98% of the adducts were stable, with 94% as BPDE-10-N^2dG. In this case, however, it was observed that the percentage of BPDE-10-N7Ade was 10 times less than that obtained with BP 7,8-dihydrodiol activated by microsomes. A logical explanation is found in the number of diastereomers in (±)-*trans*-BP 7,8-dihydrodiol, which upon epoxidation potentially yields four BPDE diastereomers, whereas the (±)-*anti*-BPDE has only two. The BPDE-10-N7Ade adduct presumably is mostly formed by one of the diastereomers not present in the BPDE preparation used.

Activation of BP by HRP or microsomes yields preponderant amounts of depurination adducts formed by one-electron oxidation, whereas BPDE and microsome-activated BP 7,8-dihydrodiol produce mainly stable adducts, in particular, BPDE-10-N^2dG.

Inhibition of Formation of BP–DNA Adducts. The inhibitory effects of DPEA and clotrimazole on cytochrome P-450 were investigated at several molar ratios of inhibitor to BP (Table IV). The relative inhibition for stable adducts was studied at all ratios, but depurination adducts were studied only at a ratio of 10:1 with DPEA and 2:1 for clotrimazole. At a molar ratio of 1:1 DPEA to BP, the inhibition of stable adducts was almost 40%, whereas at ratios of 5 and 10 it was virtually complete. The same virtually complete inhibition was achieved with 2× clotrimazole (Figure 8), and 40% inhibition was observed with

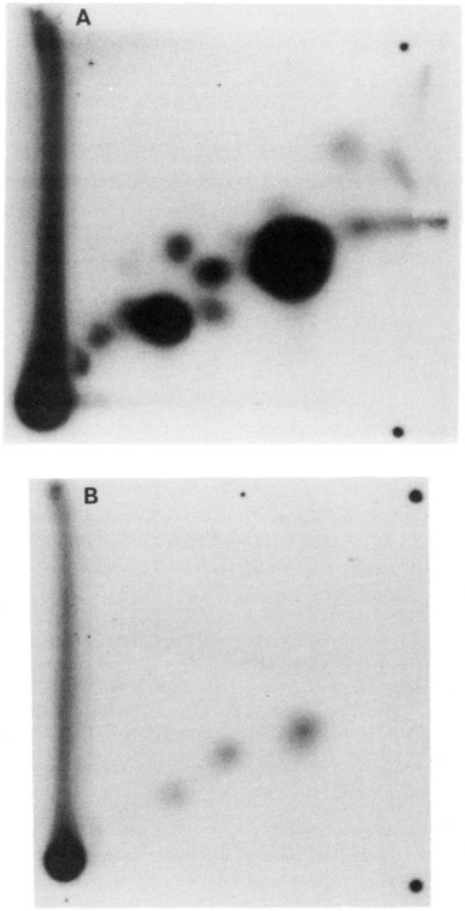

Figure 8. (A) Autoradiogram of ^{32}P-postlabeled DNA containing BP adducts formed after microsomal activation. The film was exposed at room temperature for 3.5 h. (B) Autoradiogram of ^{32}P-postlabeled DNA containing BP adducts formed after microsomal activation in the presence of 2× clotrimazole. The film was exposed at room temperature for 2 h.

0.2× clotrimazole. Formation of the depurination adducts was inhibited totally or to levels below the detection limits with either 10× DPEA or 2× clotrimazole.

Conclusions

The major mechanism of binding of BP to DNA by MC-induced rat liver microsomes is one-electron oxidation, forming adducts primarily at the N-7 of Gua and Ade and the C-8 of Gua. The BP–DNA adducts formed by this mechanism are lost from DNA by depurination. In contrast, BPDE forms mainly one stable adduct, with binding at the 2-amino of dG, and a small amount of a depurination adduct with binding at the N-7 of Ade. Only a trace (0.5%) of this BPDE-10-N7Ade adduct is found when BP is bound to DNA by microsomes. When BP 7,8-dihydrodiol is bound to DNA by microsomes, the depurination adduct BPDE-10-N7Ade constitutes about 20% of the overall adducts, but a very small amount (1.8%) is found after reaction of BPDE itself with DNA. BPDE-10-N7Gua is not detected in any of the three binding systems, namely, BP or BP-7,8-dihydrodiol activated by microsomes and BPDE reacted with DNA.

Completion of these analyses would include identification of some or all of the stable adducts detected by the ^{32}P-postlabeling technique. These constitute 4% (Table III) of the total in the microsome-catalyzed binding of BP to DNA. With all of the standard adducts available in our laboratory, we expect that some of these adducts can be identified.

In terms of quantitating the stable and depurination adducts, we think this is the most complete and accurate analysis currently possible. Only future technological advances might improve these analyses.

We are currently completing the identification and quantitation of DNA adducts formed when mouse skin is treated in vivo with BP. The pattern of BP–DNA adducts found is very similar to that observed in the microsome-catalyzed reaction.[2] These findings indicate that the effects of both stable and depurination adducts need to be investigated to learn the biological significance of BP adduction to initiation of cancer.

Acknowledgment. This research was supported by U.S. Public Health Service Grants R01-CA44686, R01-CA25176, and P01-CA49210, awarded to both research groups. Core support at the Eppley Institute was from the National Cancer Institute (P30-CA36727). Ames Laboratory is operated for the U.S. Department of Energy at Iowa State University under Contract W-7405-Eng-82, and research at Ames Laboratory was also supported by the U.S. Office of Health and Environmental Research.

References

(1) Cavalieri, E., and Rogan, E. (1985) Role of radical cations in aromatic hydrocarbon carcinogenesis. *Environ. Health Perspect.* **64**, 69–84.

(2) Cavalieri, E. L., and Rogan, E. G. (1990) Radical cations in aromatic hydrocarbon carcinogenesis. *Free Radical Res. Commun.* **11**, 77–87.

(3) Sims, P., and Grover, P. L. (1981) Involvement of dihydrodiols and diol epoxides in the metabolic activation of polycyclic hydrocarbons other than benzo[a]pyrene. In *Polycyclic Hydrocarbons and Cancer* (Gelboin, H. V., and Ts'o, P. O. P., Eds.) pp 117–181, Academic Press, New York.

(4) Conney, A. H. (1982) Induction of microsomal enzymes by foreign chemicals and carcinogenesis by polycyclic aromatic hydrocarbons: G. H. A. Clowes Memorial Lecture. *Cancer Res.* **42**, 4875–4917.

(5) Sims, P. Grover, P.L., Swaisland, A., Pal, K., and Hewer, A. (1974) Metabolic activation of benzo(a)pyrene proceeds by a diol-epoxide. *Nature (London)* **252**, 326–328.

(6) Jeffrey, A. M., Jennette, K. W., Blobstein, S. H., Weinstein, I. B., Beland, F. A., Harvey, R. G., Kasai, H., Miura, I., and Nakanishi, K. (1976) Benzo(a)pyrene–nucleic acid derivative found in vivo: Structure of a benzo(a)pyrenetetrahydrodiol epoxide–guanosine adduct. *J. Am. Chem. Soc.* **98**, 5714–5715.

(7) Cavalieri, E. L., Rogan, E. G., Devanesan, P. D., Cremonesi, P., Cerny, R. L., Gross, M. L., and Bodell, W. J. (1990) Binding of benzo[a]pyrene to DNA by cytochrome P-450-catalyzed one-electron oxidation in rat liver microsomes and nuclei. *Biochemistry* **29**, 4820–4827.

(8) Koreeda, M., Moore, P. D., Wislocki, P. G., Levin, W., Conney, A. H., Yagi, H., and Jerina, D. M. (1978) Binding of benzo[a]-pyrene 7,8-diol-9,10-epoxides to DNA, RNA and protein of mouse skin occurs with high stereoselectivity. *Science (Washington, D.C.)* **199**, 778–781.

(9) Rogan, E. G., RamaKrishna, N. V. S., Higginbotham, S., Cavalieri, E. L., Jeong, H., Jankowiak, R., and Small, G. J. (1990) Identification and quantitation of 7-(benzo[a]pyren-6-yl)guanine in the urine and feces of rats treated with benzo[a]pyrene. *Chem. Res. Toxicol.* **3**, 441–444.

(10) Rogan, E., Cavalieri, E., Tibbels, S., Cremonesi, P., Warner, C., Nagel, D., Tomer, K., Cerny, R., and Gross, M. (1988) Synthesis and identification of benzo[a]pyrene–guanine nucleoside adducts formed by electrochemical oxidation and by horseradish peroxidase catalyzed reaction of benzo[a]pyrene with DNA. *J. Am. Chem. Soc.* **110**, 4023–4029.

(11) RamaKrishna, N. V. S., Gao, F., Padmavathi, N. S., Cavalieri, E. L., Rogan, E. G., Cerny, R. L., and Gross, M. L. (1992) Model adducts of benzo[a]pyrene and nucleosides formed from its radical cation and diol epoxide. *Chem. Res. Toxicol.* (preceding paper in this issue).

[2] Unpublished results.

(12) Jankowiak, R., and Small, G. J. (1991) Fluorescence line narrowing: A high-resolution window on DNA and protein damage from chemical carcinogens. *Chem. Res. Toxicol.* **4**, 256–269.
(13) *NIH Guidelines for the Laboratory Use of Chemical Carcinogens* (1981) NIH Publication No. 81-2385, U.S. Government Printing Office, Washington, DC.
(14) Bodell, W. J., Devanesan, P. D., Rogan, E. G., and Cavalieri, E. L. (1989) ^{32}P-Postlabeling analysis of benzo[*a*]pyrene–DNA adducts formed in vitro and in vivo. *Chem. Res. Toxicol.* **2**, 312–315.
(15) Zamzow, D., Jankowiak, R., Cooper, R. S., Small, G. J., Tibbels, S. R., Cremonesi, P., Devanesan, P., Rogan, E. G., and Cavalieri, E. L. (1989) Fluorescence line narrowing spectrometric analysis of benzo[*a*]pyrene–DNA adducts formed by one-electron oxidation. *Chem. Res. Toxicol.* **2**, 29–34.
(16) Lu, P., Jeong, H., Jankowiak, R., Small, G. J., Kim, S. K., Cosman, M., and Geacintov, N. E. (1991) Comparative laser spectroscopic study of DNA and polynucleotide adducts from the (+)-*anti*-diol epoxide of benzo[*a*]pyrene. *Chem. Res. Toxicol.* **4**, 58–69.
(17) Jeong, H. (1991) Ph.D. Dissertation, Iowa State University.
(18) Sage, E., and Haseltine, W. A. (1984) High ratio of alkali-sensitive lesions to total DNA modification induced by benzo[*a*]-pyrene diol epoxide. *J. Biol. Chem.* **259**, 11098–11102.

Additions and Corrections

Roles of the Vinyl Chloride Oxidation Products 2-Chlorooxirane and 2-Chloroacetaldehyde in the in Vitro Formation of Etheno Adducts of Nucleic Acid Bases [Volume 5, Number 1, January/February 1992, pp 2–5]. F. PETER GUENGERICH

Page 2. The title should read Roles of the Vinyl Chloride Oxidation Products 1-Chlorooxirane and 2-Chloroacetaldehyde in the in Vitro Formation of Etheno Adducts of Nucleic Acid Bases.